FORMULATION AND EVALUATION OF IMMUNOMODULATORY NANONEUTRACEUTICALS

Sachin M. Kokate[1]*, Amjad Khan Pathan[2], Rajanikant T. Kakade[3]

1Department of Pharmacy, Research Scholar, Shri Jagdishprasad Jhabarmal Tibrewala University (SJJTU), Vidyanagari, Jhunjhunu, Rajasthan - 333010

2Department of Pharmacy, Professor, Shri Jagdishprasad Jhabarmal Tibrewala University (SJJTU), Vidyanagari, Jhunjhunu, Rajasthan - 333010

3Department of Pharmacy, Professor, Shri Jagdishprasad Jhabarmal Tibrewala University (SJJTU), Vidyanagari, Jhunjhunu, Rajasthan - 333010

Corresponding Author: Mr. Sachin M. Kokate*

Department of Pharmacy, Research Scholar, Shri Jagdishprasad Jhabarmal Tibrewala University (SJJTU), Vidyanagari, Jhunjhunu, Rajasthan - 333010

Abstract

Main focus of our present study is the creation and evaluation of immunomodulating nanoneutraceuticals using Gymnema sylvestre extract. A complete preformulation research was conducted to evaluate the stability, purity, and physicochemical characteristics of the extract including solubility, melting point, UV spectroscopic features, FTIR spectrum analysis, and DSC thermograms. Solubility tests revealed improved solubility in pH 7.4 phosphate buffer, which implied increased bioavailability under physiological conditions. These were nanosponges (NFs), developed and evaluated for particle size, polydispersity index (PDI), entrapment efficiency (EE%), and drug loading (DL%). G7 showed among the formulations most favorable properties suggesting its potential for effective drug delivery with the lowest PDI (0.119), smallest particle size (118 nm), and best entrapment effectiveness (96%). Important formulation components affecting the nanoparticle properties were found by statistical study using ANOVA for the quadratic model, therefore guaranteeing model dependability and repeatability. Presenting a potential quick immunomodulation solution, the ideal formulation reveals as a nanoneutraceutical stability, improved encapsulation efficiency, and desired particle properties.

Keywords: Immunomodulatory nanoneutraceuticals, Gymnema sylvestre, Nano sponges, entrapment efficiency, bioavailability, statistical optimization, ANOVA, etc.

1. Introduction

The immune system is very crucial for protection of the body against infections, diseases, and outside invaders. Other factors, like stress, aging, environmental pollutants, and a poor diet, might nonetheless compromise immune system and raise susceptibility to infections and chronic illnesses. [1-5] since immunomodulation medications may either increase or decrease immunological reactivity, thus improving overall health, they have drawn a lot of attention

recently. Derived from natural bioactive compounds, nutraceuticals—which possess safety, efficacy, and therapeutic potential—have attracted attention as promising opportunities for immunological control. Nanotechnology has changed the field of medicine delivery by increasing bioavailability, stability, and focused dispersion of bioactive compounds. [6-9] Called nanoneutraceuticals, adding nanotechnology to nutraceuticals formulations demonstrates higher efficacy than conventional nutraceuticals. These nanoscale formulations maximize the immunomodulation effects by improving the solubility, permeability, and controlled release of bioactive chemicals. Many nanocarriers: liposomes, polymeric nanoparticles, solid lipid nanoparticles, and Nano emulsions have been investigated for efficient delivery of immunomodulation medicines. [10-13]

The aim of this effort is to synthesis and evaluate very therapeutic potential immunomodulation nanoneutraceuticals. Evaluated for the created nanoneutraceuticals will be their physicochemical properties, stability, and biological efficacy in lowering immune responses. Fresh concepts for immunological wellness and disease prevention will let functional foods and nutraceuticals develop in line with this research.

2. Materials and Method

A. Materials

I. List of instruments:

Melting points of all compounds were determined in melting point apparatus. Wavelength was measured by JASCO V-530, UV-VIS Spectrophotometer. FTIR study was done using JASCO - 460 plus FT/IR. Drug release study was done using Diffusion cell apparatus DBK INSTRUMENTS Mumbai-60.

II. List of Chemicals:

The chemicals used in the formulation included Gymnema sylvestre extract powder, which was sourced from Himalaya Herbal, and ethyl cellulose, obtained from Ashland Pvt. Ltd.. Polyvinyl alcohol (PVA) was supplied by Merck Pvt. Ltd., while dichloromethane was procured from Cosmo Chem Pvt. Ltd... These chemicals were used as received without further purification unless specified.

B. Method

I. Formulation of (NFs) Nano sponges by Emulsion solvent diffusion method [14-15]

Emulsion solvent diffusion method was used to formulate. Loaded Nano sponges by using a suitable polymer i.e. Ethyl cellulose. Dispersed phase consists of specified amount of drug and polymer which was dissolved in 20 ml of an organic solvent, dichloromethane. Aqueous phase consists of specified amount of poly vinyl alcohol dissolved in 100 ml distilled water. Disperse phase was added drop by drop into aqueous phase by stirring on magnetic stirrer at 1000 rpm for about 2 hours. The Nano sponges formed were collected by filtration and dried in oven at 40°C for about 24 hours. They were then kept in the vacuum desiccators to remove the residual solvent.

II. Optimization of Formulation: [16-17]

Experimental design for nanosponge formulation

Generally, the design and optimization of the formulations is the crucial step after QbD. In this study, the nanosponge formulations were designed using CCD, a two-level full factorial design with the added center and axial points in the Response Surface Methodology (RSM) by Design Expert-13. Various concentrations of Ethyl cellulose(X1), PVA(X2) magnetic stirrer time and were employed as control variables (process parameters). Entrapment efficiency (EE %) (Y1) and Drug Loading (DL %) (Y2) were considered dependent variables. All the possible combinations of formulations were prepared by considering levels-1 and+1 for both controlled variables.

Table 1 Levels of independent variables with their transformed values in the preparation of nanosponge.

Independent Variables	Unit	Low Actual	High Actual	Low Coded	High Coded
Ethyl cellulose (A)	mg	250	700	-1.000	1.000
PVA (B)	%	1	2	-1.000	1.000
Magnetic stirrer time(C)	min	800	1000	-1.000	1.000

Table 2 Model fitting with Entrapment efficiency (EE %)

And Drug loading (DL %)

Response	Name	Units	Analysis	Minimum	Maximum	Mean	Std. Dev.	C.V %	Model
Y1	EE	%	Polynomial	76	97	86.18	3.33	3.86	Quadratic
Y2	DL	%	Polynomial	5.5	9	6.87	0.5698	8.29	Linear

Table 3 DOE suggested batches of

Gymnema sylvestre powder extract loaded nanosponges

Formulation code	Gymnema sylvestre extract(m g)	ethyl cellulose(m g)	PVA (%)	Magnetic stirrer time (rpm)	Dichloromethane(ml)
G1	5	475	1.5	1068.18	20
G2	5	475	1.5	731.821	20

G3	5	700	2	1000	20
G4	5	700	2	800	20
G5	5	250	1	1000	20
G6	5	700	1	1000	20
G7	5	853.403	1.5	900	20
G8	5	475	0.659104	900	20
G9	5	475	2.3409	900	20
G10	5	96.5966	1.5	900	20
G11	5	700	1	800	20
G12	5	475	1.5	900	20
G13	5	250	2	1000	20
G14	5	250	1	800	20
G15	5	250	2	800	20

III. Preformulation Study: [18-20]

1. Organoleptic properties:

- **Appearance and pH:**

Visually observed. A digital pH meter was used to determine the pH. The appearance and pH of a substance, such as Gymnema sylvestre extract powder, are crucial parameters in evaluating its quality and suitability for use in various applications. The appearance of the powder was visually observed to assess its physical characteristics, such as color, texture, and consistency. For Gymnema sylvestre extract powder, it was noted to have an off-white color, which is a typical feature of plant-derived powders.

- **Colour:**

A small amount of drug was placed in butter paper and viewed in a well-illuminated area. The color of a substance, such as the Gymnema sylvestre extract powder, is an important physical property that can provide initial insights into its quality and purity. To assess the color, a small amount of the powder was carefully placed on a piece of butter paper, a commonly used surface for visual inspection due to its clean, smooth texture.

- **Odour:**

Very small quantity of drug was used to get Odour. To assess the odor of Gymnema sylvestre extract powder, a very small quantity of the drug was carefully measured and placed in a container. In the case of Gymnema sylvestre, the odor was found to be odorless.

2. Solubility

The solubility of the Gymnema sylvestre drug was determined by taking small quantity of drug (approx. 10 mg) in the 10 ml volumetric flasks separately and added the 10 ml of the solvent (water, ethanol, methanol, 0.1N HCL, 0.1N NaOH, chloroform and 7.4 pH buffer) Shake vigorously and kept for some time.

3. Melting point

Melting point of Gymnema sylvestre was determined by using Thieles tube apparatus containing liquid paraffin. A capillary tube sealed at its one end and filled with small amount of drug. The capillary tube was tied to the thermometer by using thread and it was suspended in the tube. Heat was supplied by burner and the point at which the Gymnema sylvestre melts was noted.

4. UV Spectroscopic Study

Determination of wavelength of maximum absorption

To determine the optimum λmax, Gymnema sylvestre powder 10 µg /mL of working standard solution was prepared i Suitable solvent and scanned in UV wavelength range of 200 -400 nm, the solution was scanned spectrophotometrically using UV visible spectrophotometer **(JASCO V-530).**

5. Calibration curve of Gymnema sylvestre extract powder

Gymnema sylvestre extract powder 10 µg/ mL standard stock solution was done by transferring precisely weighed 10 mg of Gymnema sylvestre extract powder to 10 ml volumetric flask and dissolved in Suitable solvent. The volume was filled up to the mark with Suitable solvent. From this solution 1 ml was precisely transferred into 10ml volumetric flask and volume was made up to the mark with Suitable solvent. A calibration curve was plotted over a concentration range of 2-10 µg/mL for Gymnema sylvestre extract powder.

6. FTIR spectroscopy [21]

FTIR spectroscopy is a powerful tool for identifying types of chemical bonds (functional groups). The wavelength of light absorbed is characteristic of the chemical bond. The IR spectra were recorded using FT-IR spectrophotometer (Jasco-450 plus, Japan) with reflectance principle. Sample preparation involved mixing the sample with KBr, triturating in glass mortar and finally placing in the sample holder. The spectra were scanned over a frequency range 4000 –400 cm-1 .The characteristic functional groups were identified from the spectra depicted in Figure.

7. Drug-excipient compatibility study [22]

Compatibility studies of active pharmaceutical ingredient (API) and excipients are essential in the Preformulation stage of the development of new dosage forms. The physical and chemical interactions between an API and the excipients might have an impact on the final product. Chemical nature, the former's stability and bioavailability, and, as a result, its therapeutic potential Efficacy and safety are two important factors to consider. The drug and excipient compatibility

should be established prior to the formulation. In a 1:1 ratio, the medicine is mixed with excipients. The mixture was kept at 37 degrees Celsius for 14 days in airtight, light-resistant containers. The samples were scanned by FTIR spectroscopy and the spectra were analyzed.

8. DSC studies [23]

DSC is a thermo analytical technique which is used to investigate various endothermic and exothermic physical transformations that occur in the test sample. It has wide applicability as a quality control tool used for measuring sample purity and interactions with other substances. The DSC thermograms were recorded using Differential scanning calorimeter (DSC 823e, Mettler Toledo, Japan). Approximately 2-5 mg of each sample was heated in a pierced aluminum pan from 30° C to 300°C at a heating rate of 10°C/min under a stream of nitrogen at flow rate of 50ml/min. Thermal data analyses of the DSC thermograms were conducted using STARe software (version 5.21) and the thermograms are depicted in Figure.

IV. Evaluation of (NFs) Nano sponges [24-28]

1. Particle size and Polydispersity index (PDI)

Samples were diluted appropriately with the aqueous phase of the formulation for the measurement. The pH of diluted samples was adjusted appropriately as required at 25ºC. A sufficient high energy input was used to break down the droplets in to the nanometer range. The Polydispersity index measured the size distribution of the nanoparticles population. The mean hydrodynamic diameter and Polydispersity index of the particles were calculated using the cumulated analysis after averaging of the total measurements.

2. Entrapment efficiency (EE %) and Drug loading (DL %)

The entrapment efficiency of Cilnidipine loaded SLN formulation was determined by centrifugation method, in which 10 mg in 10 ml of the prepared SLN suspension was placed in the Eppendorf for centrifugation (RM-12) at 1400 rpm for 30min after centrifugation, the supernatant liquid was separated, containing the un-entrapped drug, diluted with phosphate buffer pH 6.8 and analyzed using UV spectrophotometer at 240 nm. By using that absorbance entrapment efficiency (%EE) and Drug Loading (%DL) are calculated by using the following formula.

$$Entrapment\ efficiency(EE\ \%) = \frac{Total\ amount\ of\ drug - Amount\ of\ the\ un\text{-}entrapped\ drug}{Total\ amount\ of\ drug} \times 100 \ldots (1)$$

$$Drug\ Loading\ (DL\%) = \frac{Actual\ drug\ content}{Weight\ of\ obtained\ product} \times 100 \ldots (2)$$

3. Differential Scanning Calorimetry (DSC) study

Thermo grams of the lyophilized powder samples of different preparation were studied. An unfilled aluminums pan was employed as a reference. DSC measurements were performed at a heating rate of 5ºC/min from 25 to 250ºC using aluminum sealed pan. The sample size was 5-10mg for each measurement. Throughout the dimension, the sample cell was flush out with

nitrogen gas. The Differential Scanning Calorimetry (DSC) analysis was conducted to investigate the thermal behavior and stability of the lyophilized powder samples from different preparations. The DSC measurements were carried out at a controlled heating rate of 5°C/min, ranging from 25°C to 250°C. This temperature range was selected to cover both the lower and higher thermal limits of the sample, ensuring the identification of any phase transitions or stability issues during the thermal analysis.

4. Field Scanning electron microscopy (FSEM) analysis

Surface morphological characteristics of freeze dried and reconstituted Nano sponges were individually evaluated with SEM. Prior to imaging, mounted freeze-dried Nano sponge's samples were sputter coated with platinum. Freeze dried Nano suspension was reconstituted with double distilled water and adsorbed on carbon tapes after appropriate dilution and tapes were allowed to dry at room temperature (25ºC) for 24 hrs. The results were compared with surface morphological characteristics of ATRC Nano sponges before freeze drying.

5. X-ray Diffraction (XRD) study

The PXRD patterns were documented on an x-ray diffractometer (X-ray generator (PW 1729) (Philips, Eindhoven, Netherlands.). The samples were irradiated with monochromatized CuKa radiation and analyzed between 2-80ºC 2Ø. The patterns were collected with voltage of 30kV and current of 30mA respectively. The scanning pace (2Ø/min-1) was set at 10 ºC/min. The Powder X-ray Diffraction (PXRD) analysis was conducted to investigate the crystallographic properties and phase transitions of the nanosponges. The PXRD patterns were obtained using an X-ray diffractometer (Philips PW 1729, Eindhoven, Netherlands) equipped with a monochromatized CuKa radiation source, which is ideal for generating precise diffraction data. The X-rays, with a wavelength of 1.5406 Å, were used to irradiate the sample.

3. Results and Discussion

1. Preformulation study

A Preformulation research was carried out to ensure that the medication and polymer were in a stable and pure state before being formulated into a dosage form also a for determinations of characteristics which may play important role in dosage form development. Preformulation research is a critical step in the development of any pharmaceutical dosage form, as it ensures that both the active pharmaceutical ingredient (API) and the excipients (such as polymers) are in a stable and pure state before formulation. This phase involves a comprehensive analysis of the physicochemical properties of the drug and polymer to identify any potential issues that could affect the stability, efficacy, or safety of the final product. The goal of preformulation is to gather essential data that will guide the design and optimization of the dosage form, ensuring that it is both effective and manufacturable.

A. Physico-chemical Characterization of Gymnema sylvestre extract powder

1. Organoleptic properties of Gymnema sylvestre extract powder:

- **Appearance and pH:** Solid
- **Colour:** off-white

- **Odor:** odorless

2. Solubility

The solubility study of *Gymnema sylvestre* extract powder across various mediums shows that the extract has the highest solubility in pH 7.4 Phosphate buffer (600 µg/mL), followed by 0.1N HCl (500 µg/mL), indicating good solubility in both neutral and acidic conditions. Moderate solubility was observed in pH 6.8 Phosphate buffer (400 µg/mL) and pH 4.5 Acetate buffer (300 µg/mL), with the lowest solubility in water (200 µg/mL). These results suggest that the extract is more soluble in environments that mimic physiological pH, which could enhance its bioavailability when administered in formulations designed for such conditions. The solubility study of Gymnema sylvestre extract powder across various mediums revealed important insights into its behavior in different pH environments. The extract demonstrated the highest solubility in pH 7.4 phosphate buffer, with a concentration of 600 µg/mL, indicating that it is most soluble in a neutral, physiological-like pH. This is particularly significant, as it suggests that the extract is likely to have enhanced bioavailability when administered in formulations intended to simulate the conditions of the human gastrointestinal tract, where pH 7.4 is common.

In contrast, the extract also showed good solubility in more acidic conditions, as evidenced by its solubility of 500 µg/mL in 0.1N hydrochloric acid (HCl). This is relevant for formulations that may be exposed to acidic environments, such as the stomach, where the pH can range from 1 to 3. Moderate solubility was observed in pH 6.8 phosphate buffer (400 µg/mL) and pH 4.5 acetate buffer (300 µg/mL), suggesting that the extract remains reasonably soluble in mildly acidic to near-neutral conditions, which are also common in various parts of the digestive system.

The lowest solubility was observed in water (200 µg/mL), which may indicate that the extract's hydrophilic properties are not as strong compared to its solubility in buffered solutions. This could imply that the extract may require the presence of specific buffering agents to enhance its solubility and subsequent absorption in the body.

Table 4 Solubility study of Gymnema sylvestre extract powder

Medium	**Solubility of Gymnema sylvestre extract powder(µg/mL)**
Water	200
0.1N HCl	500
pH4.5 Acetate buffer	300
pH6.8 Phosphate buffer	400
pH7.4 Phosphate buffer	600

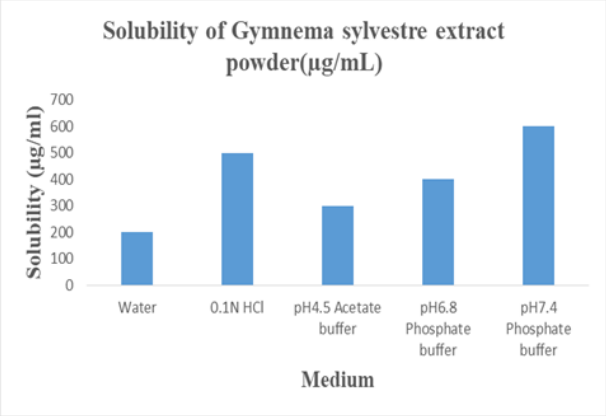

Figure 1 Solubility study of Gymnema sylvestre extract powder

3. Melting point determination:

Table 5 Melting point of Gymnema sylvestre extract powder

Sr. No.	Sample	Melting point	Reported
1.	Gymnema sylvestre extract	152℃	151-175℃

The melting point of Gymnema sylvestre extract was found to be 152°C, which falls within the reported range of 151-175°C.

B. UV Spectroscopic Study

a. Determination of wavelength of maximum absorption

Discussion: The standard solutions containing Gymnema sylvestre extract powder 1 µg/ml was scanned in UV range 200-400 nm using water as blank. The wavelength corresponding to maximum absorbance in water was found to be 370 nm.

Table 6 Calibration curve observation of Gymnema sylvestre powder

Sr. No.	Concentration (mgm/ml)	Absorbance
1	10	0.02
2	20	0.058
3	30	0.097

4	40	0.141
5	50	0.185

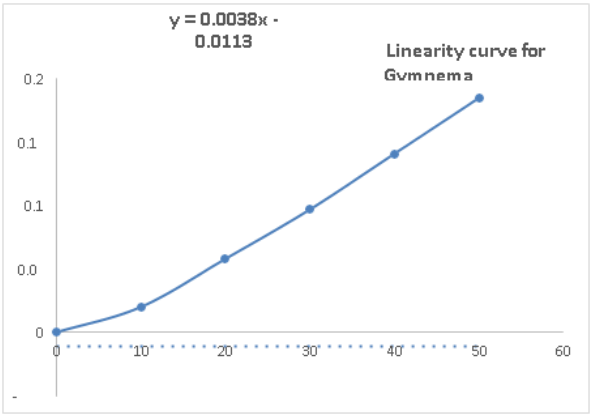

Figure 2 Calibration curve of Gymnema sylvestre extract powder

b. FT-IR spectroscopy study:

The spectrum interpretation of Gymnema sylvestre extract powder reveals a variety of functional groups, reflecting the extract's composition and potential bioactivity. The O– H stretch is observed at 3625.52 cm^{-1} and 3646.73 cm^{-1}, which aligns with the reported range of 3640–3610 cm^{-1}, indicating the presence of hydroxyl groups. Additionally, C– H stretches appear at 2864.74 cm^{-1} and 2932.23 cm^{-1}, corresponding to the typical range of 3000–2850 cm^{-1}. A notable C=O stretch at 1713.44 cm^{-1} is slightly lower than the reported range of 1760–1690 cm^{-1}, suggesting carbonyl functionalities. Furthermore, C=C stretches are detected at 1680.66 cm^{-1} and 1650.77 cm^{-1}, fittingwithin the reported range of 1680–1640 cm^{-1}. The presence of N–O asymmetric stretches is indicated at 1555.31 cm^{-1}, 1538.92 cm^{-1}, and 1504.2 cm^{-1}, aligning with the reported range of 1550–1475 cm^{-1}. Other functional groups include a C–H bend at 1454.06 cm^{-1}, near the reported 1470–1450 cm^{-1} range, and C–N stretches at 1291.11 cm^{-1}, close to the reported range of 1335–1250 cm^{-1}. Lastly, C=H bends are noted at 925.664 cm^{-1} and 797.421 cm^{-1}, consistent with the reported range of 1000–650 cm^{-1}. This analysis underscores the extract's diverse functional groups, supporting its potential therapeutic applications.

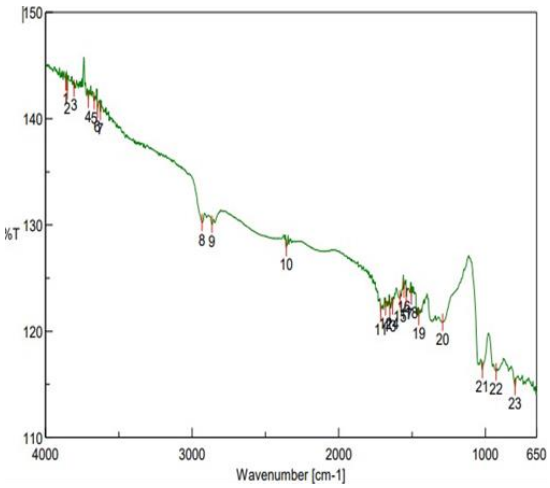

Figure 3 FTIR Spectra of Gymnema sylvestre extract powder

No.	Position	Intensity	No.	Position	Intensity
1	3861.76	143.448	2	3852.11	142.611
3	3805.83	142.865	4	3708.44	141.801
5	3667.94	141.653	6	3646.73	140.86
7	3625.52	140.641	8	2932.23	130.224
9	2864.74	130.054	10	2358.52	127.837
11	1713.44	121.78	12	1680.66	122.275
13	1650.77	122.147	14	1633.41	122.363
15	1582.31	123.05	16	1555.31	123.957
17	1538.92	123.248	18	1504.2	123.294
19	1454.06	121.378	20	1291.11	120.831
21	1020.16	116.364	22	925.664	116.18
23	797.421	114.783			

Table 7 Spectrum interpretation of Gymnema sylvestre extract powder

Function group	Observed Wave number(cm^{-1})	Reported Wave number(cm^{-1})
O–H stretch	3625.52,3646.73,	3640–3610
C–H stretch	2864.74, 2932.23	3000–2850
	2358.52	
C=O stretch	1713.44	1760–1690
–C=C– stretch	1680.66,1650.77	1680–1640

N–O asymmetric stretch	1555.31, 1538.92,1504.2	1550–1475
C–H bend	1454.06	1470–1450
C–N stretch	1291.11	1335–1250
=C–H bend	925.664,797.421	1000–650

4. DSC Studies

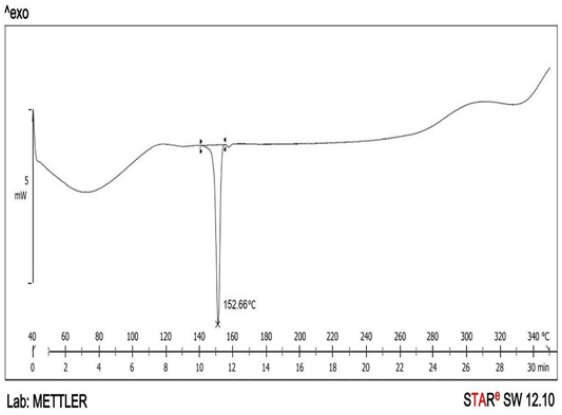

Figure 4 Spectrum of DSC of Gymnema sylvestre extract powder

DSC graph of pure Gymnema sylvestre extract powder showing end set at 152.66°C, which corresponding to the reported temperature in the literature survey. It confirms the purity of Gymnema sylvestre. The Differential Scanning Calorimetry (DSC) analysis of pure Gymnema sylvestre extract powder revealed an endothermic peak at 152.66°C, which closely matches the reported melting point of 152°C in the literature. This sharp endothermic peak indicates the specific temperature at which the extract undergoes phase transition, which is typically associated with the melting of a substance.

- **Post formulation study**

Evaluation of (NFs) Nanosponges

1. Particle size and Polydispersity index (PDI)

The particle size of the nanosponges across the formulations ranges from 118 nm (G7) to 175 nm (G8). Formulation G7, with the smallest particle size of 118 nm, is likely to offer a better surface area and potentially enhanced drug release characteristics. Conversely, G8, with the largest particle size of 175 nm, may exhibit different drug release kinetics or altered stability. Regarding the Polydispersity Index (PDI), values vary from 0.119 (G7) to 0.95 (G2), indicating different levels of homogeneity in particle size distribution. A lower PDI, such as 0.119 in G7, signifies a more uniform particle size distribution, which is generally preferable for consistent drug delivery and

stability. On the other hand, a higher PDI, like 0.95 in G2, suggests a broader size distribution, potentially leading to variability in drug release and aggregation issues.

Table 8 Particle size and Polydispersity Index of Nano sponges

Formulation code	Particle size (nm)	Polydispersity index (PDI).
G1	134.56	0.365
G2	125	0.95
G3	124.87	0.298
G4	118.29	0.59
G5	124	0.61
G6	120	0.654
G7	118	0.119
G8	175	0.245
G9	119	0.125
G10	121	0.789
G11	129	0.658
G12	134	0.871
G13	139	0.78
G14	127	0.45
G15	129.8	0.487

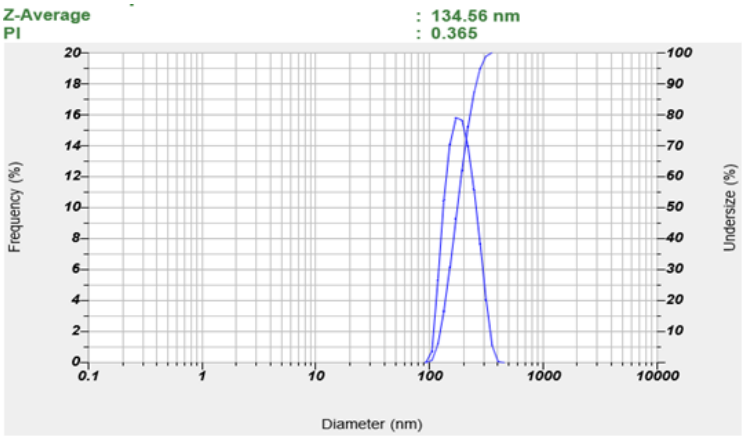

Figure 5 Particle size and Polydispersity Index (PDI) of G1

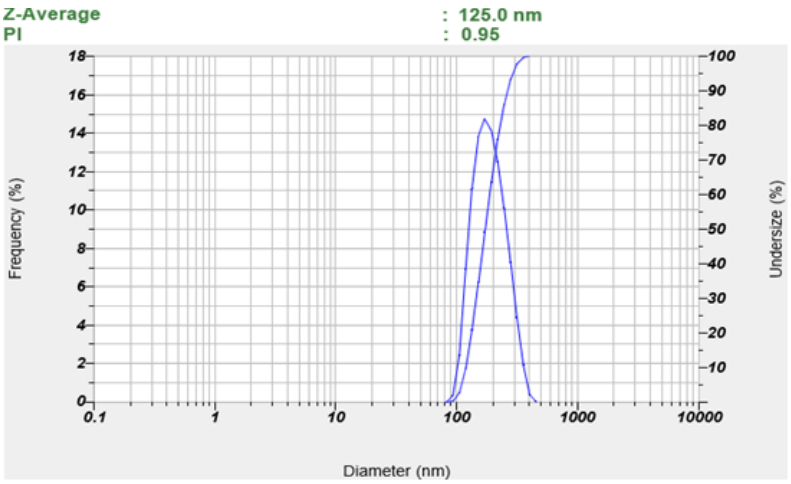

Figure 6 Particle size and Polydispersity Index (PDI) of G2

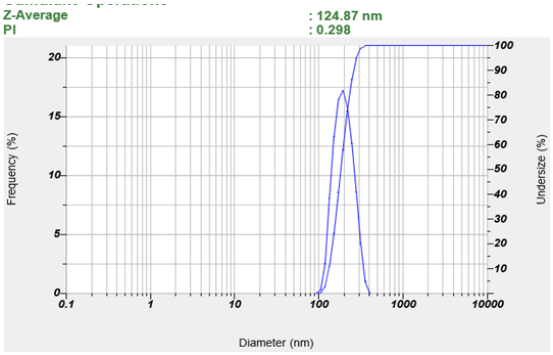

Figure 7 Particle size and Polydispersity Index (PDI) of G3

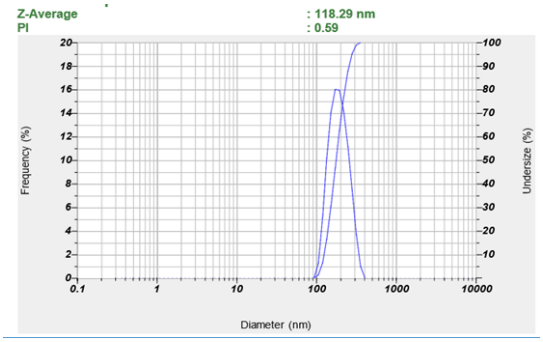

Figure 8 Particle size and Polydispersity Index (PDI) of G4

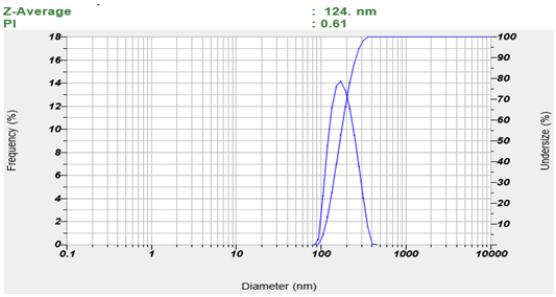

Figure 9 Particle size and Polydispersity Index (PDI) of G5

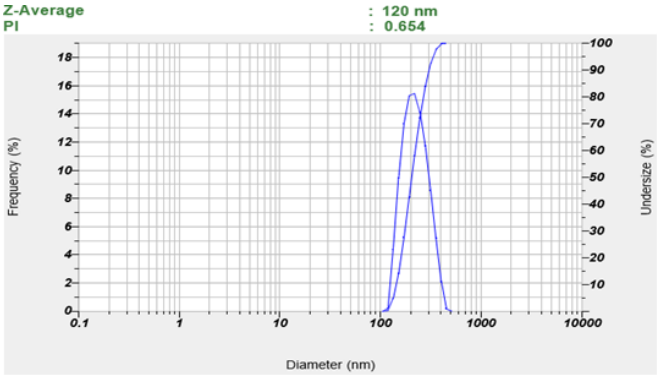

Figure 10 Particle size and Polydispersity Index (PDI) of G6

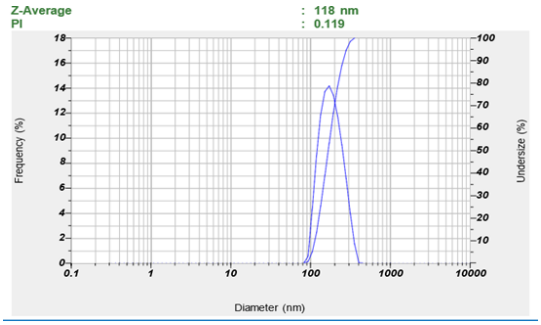

Figure 11 Particle size and Polydispersity Index (PDI) of G7

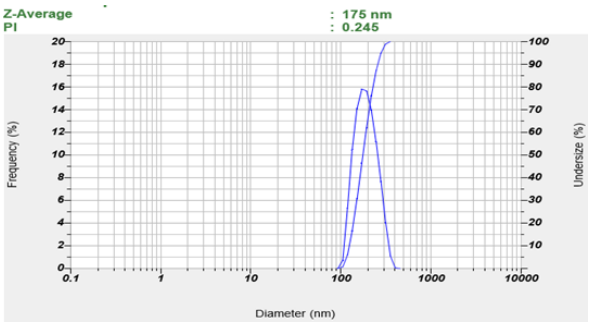

Figure 12 Particle size and Polydispersity Index (PDI) of G8

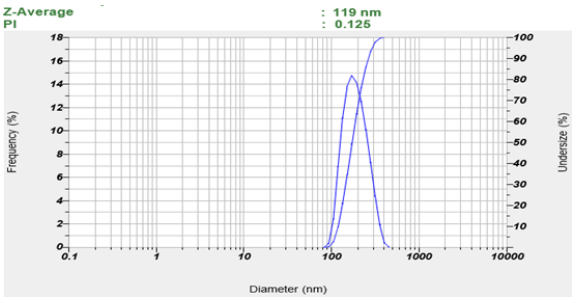

Figure 13 Particle size and Polydispersity Index (PDI) of G9

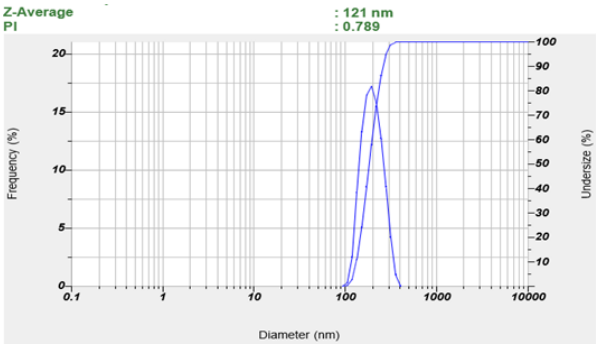

Figure 14 Particle size and Polydispersity Index (PDI) of G10

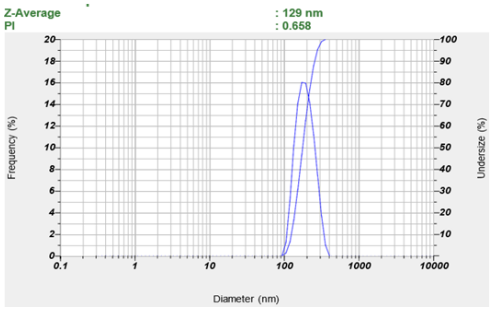

Figure 15 Particle size and Polydispersity Index (PDI) of G11

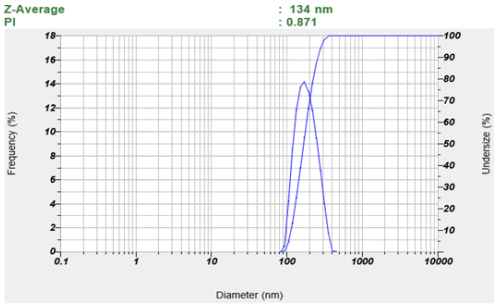

Figure 16 Particle size and Polydispersity Index (PDI) of G12

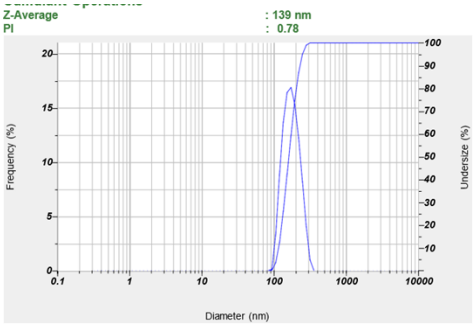

Figure 17 Particle size and Polydispersity Index (PDI) of G13

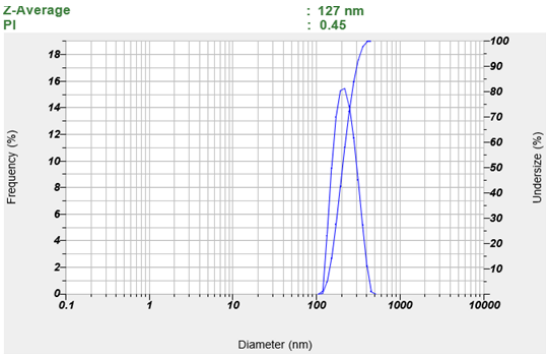

Figure 18 Particle size and Polydispersity Index (PDI) of G14

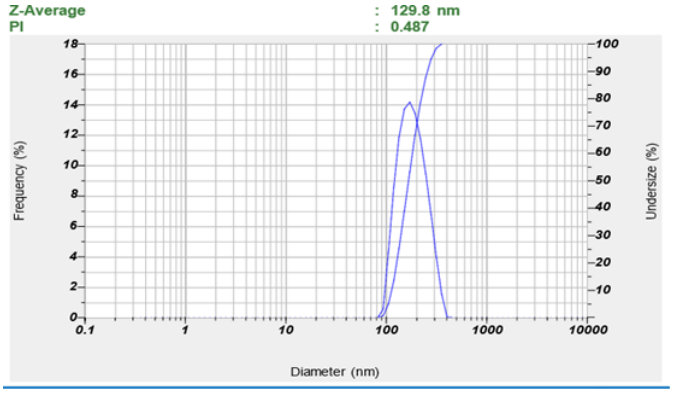

Figure 19 Particle size and Polydispersity Index (PDI) of G15

2. Entrapment efficiency (EE %) and drug loading (DL %):

The entrapment efficiency (EE %) of formulations G1 to G15 shows a range from 76% to 96%, with the highest values observed in formulations G7 (96%) and G6 (95%), followed by G11 (95%). These formulations demonstrate superior encapsulation of the active ingredient, which is crucial for ensuring effective drug delivery and sustained release. Formulations with lower EE%, such as G12 (76%), G5 (78%), and G15 (80.86%), may require optimization to improve their ability to retain the drug within the delivery system. Overall, G7 stands out as the most optimized formulation, exhibiting both high drug loading and high entrapment efficiency, making it the best candidate for further development.

Table 9 Entrapment efficiency (EE %) of G1- G15

Sr.no	Entrapment efficiency (EE %)
G1	89
G2	86
G3	90
G4	85

G5	78
G6	95
G7	96
G8	82.89
G9	82
G10	88
G11	95
G12	76
G13	81
G14	88
G15	80.86

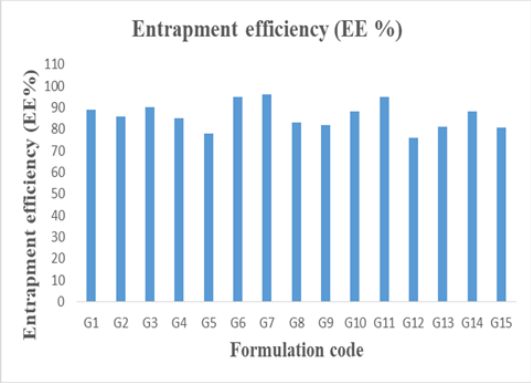

Figure 20 Entrapment efficiency of Nanosponge containing Gymnema sylvestre

ANOVA for Quadratic model

Response 1: Entrapment efficiency

Source	Sum of Squares	df	Mean Square	F-value	p-value	
Model	**481.11**	**9**	**53.46**	**4.82**	**0.0491**	**significant**
A-Ethyl Cellulose	**182.42**	**1**	**182.42**	**16.44**	**0.0098**	
B-PVA	34.28	1	34.28	3.09	0.1391	
C-Magnetic stirrer time	0.1029	1	0.1029	0.0093	0.9270	

AB	17.58	1	17.58	1.58	0.2637	
AC	31.44	1	31.44	2.83	0.1531	
BC	24.99	1	24.99	2.25	0.1937	
A^2	163.05	1	163.05	14.70	0.0122	
B^2	23.94	1	23.94	2.16	0.2018	
C^2	86.30	1	86.30	7.78	0.0385	
Residual	55.48	5	11.10			
Cor Total	536.59	14				

Factor coding is coded.

Sum of squares is Type III – Partial

The Model F-value of 4.82 implies the model is significant. There is only a 4.91% chance that an F-value this large could occur due to noise.

P-values less than 0.0500 indicate model terms are significant. In this case A, A^2, C^2 are significant model terms. Values greater than 0.1000 indicate the model terms are not significant. If there are many insignificant model terms (not counting those required to support hierarchy), model reduction may improve your model.

Fit Statistics

Std. Dev.	**3.33**		**R^2**	**0.8966**
Mean	**86.18**		**Adjusted R^2**	**0.7105**
C.V. %	**3.86**		**Predicted R^2**	**-0.4055**
			Adeq Precision	**7.6575**

A negative Predicted R^2 implies that the overall mean may be a better predictor of your response than the current model. In some cases, a higher order model may also predict better.

Adeq Precision measures the signal to noise ratio. A ratio greater than 4 is desirable. Your ratio of 7.658 indicates an adequate signal. This model can be used to navigate the design space.

Final Equation in Terms of Coded Factors

Entrapment efficiency	**=**
+76.21	
+3.65	A

-1.58	B
+0.0868	C
-1.48	AB
+1.98	AC
+1.77	BC
+5.19	A^2
+1.99	B^2
+3.78	C^2

The equation in terms of coded factors can be used to make predictions about the response for given levels of each factor. By default, the high levels of the factors are coded as +1 and the low levels are coded as -1. The coded equation is useful for identifying the relative impact of the factors by comparing the factor coefficients.

Final Equation in Terms of Actual Factors.

Entrapment efficiency	=
+495.34481	
-0.140685	Ethyl Cellulose
-52.58856	PVA
-0.773674	Magnetic stirrer time
-0.013178	Ethyl Cellulose * PVA
+0.000088	Ethyl Cellulose * Magnetic stirrer time
+0.035350	PVA * Magnetic stirrer time
+0.000103	Ethyl $Cellulose^2$
+7.95479	PVA^2
+0.000378	Magnetic stirrer $time^2$

The equation in terms of actual factors can be used to make predictions about the response for given levels of each factor. Here, the levels should be specified in the original units for each factor. This equation should not be used to determine the relative impact of each factor because the coefficients are scaled to accommodate the units of each factor and the intercept is not at the center of the design space.

Counter plot of entrapment efficiency:

A counter plot is typically used to visualize how independent variables (factors) influence a dependent variable (entrapment efficiency) while keeping other factors constant. Each axis of the counter plot represents one of the two independent variables. The optimized batch, for the region on the counter plot where the entrapment efficiency is maximized. This region is represented by contour lines, and the highest contour line indicates the highest entrapment efficiency achievable under the given conditions.

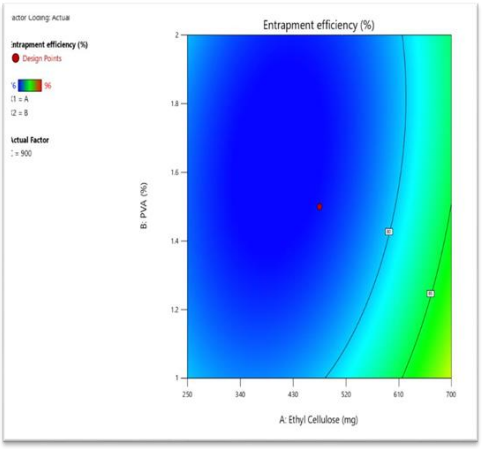

Figure 21 Counter plot of entrapment efficiency 3D response plot of entrapment efficiency:

A 3D response curve is a representation of how two independent variables influence dependent variable (entrapment efficiency) in three dimensions. In the 3D response curve, the two independent variables are typically represented on the X and Y axes, while the entrapment efficiency (the response variable) is represented on the Z axis, forming a three-dimensional plot. The optimized batch on the 3D response curve, look for the peak or highest point on the curve. The coordinates (values of the two factors) corresponding to this peak represent the ideal conditions for achieving the maximum entrapment efficiency.

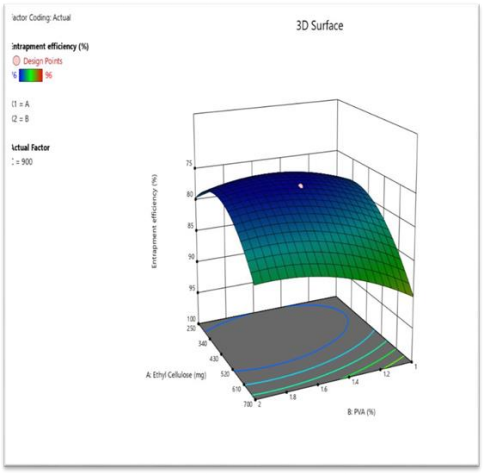

Figure 22 3D response plot of entrapment efficiency

Drug loading (DL %):

Among G1–G15, Formulation G7 seems to be the most effective in combining the active pharmaceutical ingredient (API) with the maximum drug loading—9%. Increased pharmaceutical loading improves bioavailability, therapeutic effectiveness, and may lower dosage frequency and thus increase patient compliance. Though G7's little advantage makes G6 (8.9% drug loading) the superior prospect for future development, stability testing, and in vivo assessment, it is nevertheless a good contender. Although both formulations show potential, G7 is the greatest option for clinical development because of its greater drug incorporation and possibilities for superior release dynamics.

Table 10 Drug loading (DL %) of G1- G15

Sr.no	Drug Loading (DL %)
G1	7
G2	5.8
G3	6.7
G4	6.6
G5	7
G6	8.9
G7	9
G8	6.8
G9	5.8
G10	5.9
G11	8.3
G12	7.1
G13	6.5
G14	6.2
G15	5.5

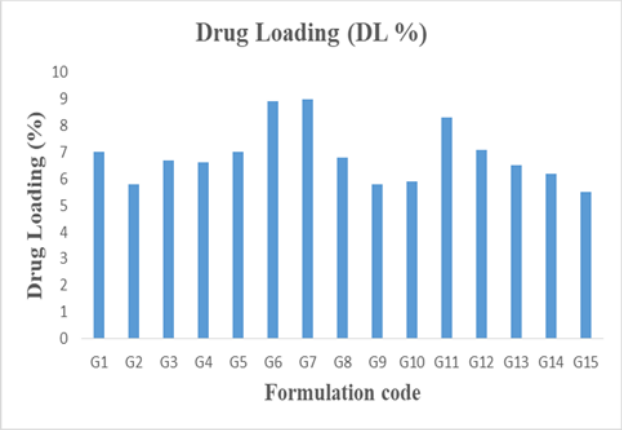

Figure 23 Drug loading (DL %) of G1- G15

ANOVA for Linear model

Response 2: Drug Loading

Source	Sum of Squares	df	Mean Square	F-value	p-value	
Model	13.02	3	4.34	13.37	0.0005	significant
A-Ethyl Cellulose	7.99	1	7.99	24.61	0.0004	
B-PVA	3.47	1	3.47	10.68	0.0075	
C-Magnetic stirrer time	1.56	1	1.56	4.81	0.0507	
Residual	3.57	11	0.3246			
Cor Total	16.59	14				

Factor coding is coded.

Sum of squares is Type III - Partial

The Model F-value of 13.37 implies the model is significant. There is only a 0.05% chance that an F-value this large could occur due to noise.

P-values less than 0.0500 indicate model terms are significant. In this case A, B are significant model terms. Values greater than 0.1000 indicate the model terms are not significant. If there are many insignificant model terms (not counting those required to support hierarchy), model reduction may improve your model.

Fit Statistics

Std. Dev.	**0.5698**		**R^2**	**0.7848**
Mean	6.87		Adjusted R^2	0.7261
C.V. %	8.29		Predicted R^2	0.5880
			Adeq Precision	10.9232

The Predicted R^2 of 0.5880 is in reasonable agreement with the Adjusted R^2 of 0.7261;

i.e. the difference is less than 0.2.

Adeq Precision measures the signal to noise ratio. A ratio greater than 4 is desirable. Your ratio of 10.923 indicates an adequate signal. This model can be used to navigate the design space.

Final Equation in Terms of Coded Factors

Drug Loading	**=**
+6.87	
+0.7648	A
-0.5039	B
+0.3382	C

The equation in terms of coded factors can be used to make predictions about the response for given levels of each factor. By default, the high levels of the factors are coded as +1 and the low levels are coded as -1. The coded equation is useful for identifying the relative impact of the factors by comparing the factor coefficients.

Final Equation in Terms of Actual Factors

Drug Loading	**=**
+3.72698	
+0.003399	Ethyl Cellulose

-1.00782	PVA
+0.003382	Magnetic stirrer time

The equation in terms of actual factors can be used to make predictions about the response for given levels of each factor. Here, the levels should be specified in the original units for each factor. This equation should not be used to determine the relative impact of each factor because the coefficients are scaled to accommodate the units of each factor and the intercept is not at the center of the design space.

Counter plot of drug loading:

A counter plot is used to visualize how two independent variables (factors) influence a dependent variable (drug loading) while keeping other factors constant. Each axis of the counter plot represents one of the two independent variables. In the optimized batch, for the region on the counter plot where drug loading is maximized. This region is represented by contour lines, and the highest contour line indicates the highest drug loading achievable under the given conditions. An optimized batch is associated with the specific combination of factor values (represented coordinates on the plot) where the highest contour line intersects. This combination of factors represents the ideal conditions that result in the highest drug loading.

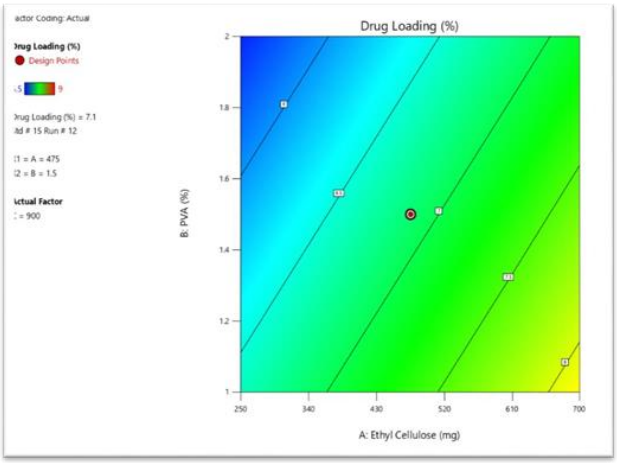

Figure 24 Counter plot of drug loading 3D

Response Plot of Drug Loading:

A 3D response plot represents how two independent variables (factors) influence a dependent variable (drug loading) in three dimensions. It allows to visualize the relationship between these variables more comprehensively the 3D response plot, the two independent variables are typically represented on the X and Y axes, while drugloading (the response variable) is represented on the Z axis, forming a three- dimensional plot. The optimized batch on the 3D response plot, for the peak or highest point on the curve. The coordinates (values of the two factors) corresponding to this peak represent the ideal conditions for achieving the maximum drug loading.

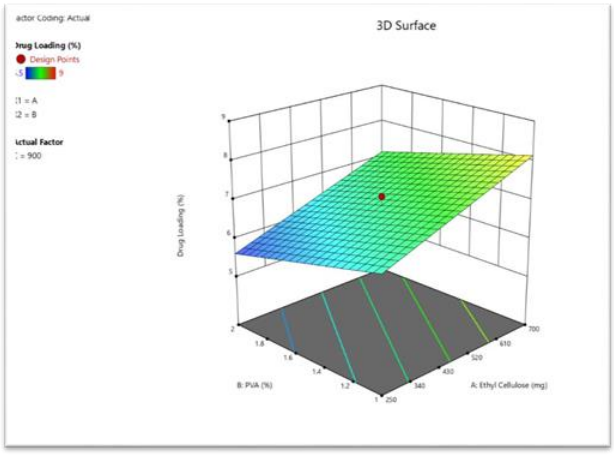

Figure 25 3D response plot of drug loading

3. Differential scanning calorimetry (DSC Study)

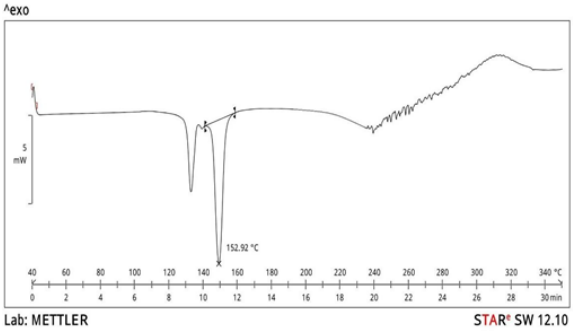

Figure 26 DSC thermogram of G7 optimized formulation

The G7 optimized formulation exhibits a significant endothermic peak at 152.92°C, indicating a crucial thermal transition, likely representing its melting point or phase change. This suggests good thermal stability, ensuring integrity under various storage and handling conditions. The formulation's ability to withstand high temperatures without degradation enhances its shelf-life, efficacy, and pharmaceutical suitability. Further studies will help correlate this thermal behavior with chemical stability, drug release, and overall formulation performance, reinforcing G7's potential for clinical and commercial applications.

4. Field emission scanning electron microscopy (FESEM)

The FESEM image of the G7 optimized formulation reveals irregularly shaped microsponges with rough surfaces, suggesting an increased surface area that may enhance drug release. The formulation exhibits a mixed size distribution, with larger aggregated particles and smaller fragments that could improve drug dissolution and bioavailability. The structural integrity remains intact, and the uniform particle distribution indicates consistency in formulation. These characteristics support controlled and sustained drug release, though further quantitative analysis (e.g., drug release kinetics and stability testing) is needed to confirm its clinical suitability.

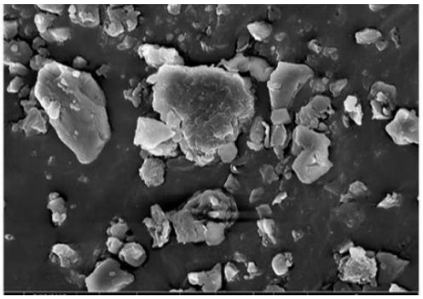

Figure 27 FESEM of G7 optimized formulation

5. X –ray diffraction study

The X-ray diffraction (XRD) pattern shows distinct peaks at 2θ values of 6.58°, 7.89°, 9.50°, 9.80°, 11.20°, 14.28°, 16.28°, 17.20°, and 19.20°, indicating the presence of crystalline phases within the sample. The sharp peaks, particularly around 9.50° and 9.80°, suggest a significant degree of crystallinity, as crystalline structures typically produce such peaks due to their orderly atomic arrangement. The decline in intensity beyond 20° suggests the presence of an amorphous phase, common in materials with mixed-phase compositions. The crystallinity observed may affect the material's properties, such as solubility, stability, and mechanical strength, which are crucial for applications like drug formulation. To accurately identify the phases present, these 2θ values would need to be compared with standard reference patterns. Overall, the XRD pattern reveals a mixture of crystalline and amorphous phases, with the crystalline regions potentially influencing the material's application in various fields.

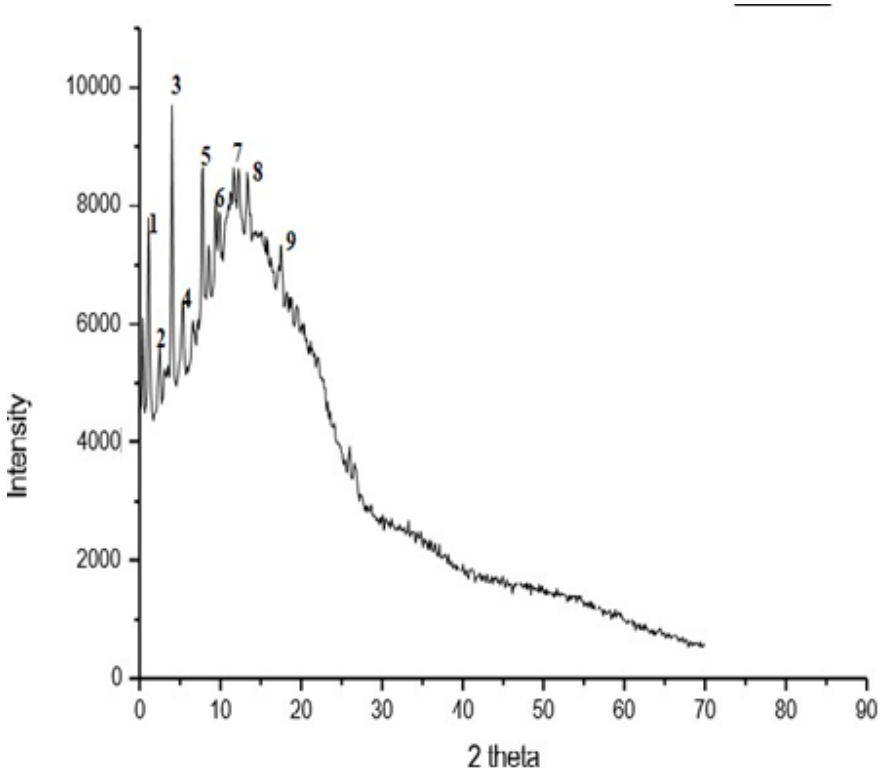

Figure 28 X-ray Diffraction of G7 optimized formulation

4. Conclusion

The present study successfully formulated and evaluated immunomodulatory nanoneutraceuticals containing Gymnema sylvestre extract. A comprehensive preformulation study confirmed the stability, purity, and physicochemical properties of the extract, including solubility, melting point, UV spectroscopic characteristics, FTIR spectral analysis, and DSC thermograms. Improved solubility in pH 7.4 phosphate buffer shown by solubility studies indicated higher bioavailability under physiological conditions.

Particle size, polydispersity index (PDI), entrapment efficiency (EE %), and drug loading (DL %) all came under impact to best make nano sponges (NFs). G7 had the lowest PDI (0.119), the smallest particle size (118 nm), and the greatest entrapment effectiveness (96%), among the developed formulations, therefore offering the best chance for successful drug distribution. Statistical study revealed important components affecting the formulation parameters by means of ANOVA for the quadratic model, therefore verifying the dependability and durability of the model. Last optimal formulation shown stability, improved encapsulation efficiency, and desired particle properties. Promising as a rapid immunomodulation nanoneutraceutical.

Acknowledgments

Conflict of interest:

The authors declare no conflict of interest.

5. References

1. Ahmed S, Khan H, Aschner M, Hasan MM, Hassan ST. Therapeutic potential of phytopharmaceuticals and functional foods in immune disorders. Food Chem Toxicol. 2020;143:111560.
2. D'Souza C, Shegokar R. Nanotechnology-based nutraceuticals for immune modulation. Appl Microbiol Biotechnol. 2022;106(4):1357-1373.
3. Dutta RK, Arya RK, Khatri P, Nair S, Ahmad A. Emerging role of nanonutraceuticals in cancer immunotherapy. J Control Release. 2021;338:436-454.
4. Mishra V, Bansal KK, Verma A, Yadav N, Thakur S, Sudhakar K, et al. Solid lipid nanoparticles: Emerging colloidal nano drug delivery systems. Pharmaceutics. 2018;10(4):191.
5. Pandey A, Vishwakarma J, Gupta AP, Kumar A, Kumar A, Gupta S. Role of nanotechnology in enhancing the bioavailability and therapeutic efficacy of herbal medicines. Biomed Pharmacother. 2021;133:111072.
6. Yadav D, Kumar N, Chauhan NS, Mishra S. Role of nanotechnology in COVID-19: Therapeutics and vaccine development. J Drug Deliv Sci Technol. 2022;67:102935.
7. Mukherjee S, Ray S, Thakur RS. Solid lipid nanoparticles: A modern formulation approach in drug delivery system. Indian J Pharm Sci. 2009;71(4):349-358.
8. Sharma AR, Bhattacharya M, Sharma G, Lee SS, Chakraborty C. Future prospects of nanotechnology in nutraceuticals: A new paradigm. J Nanobiotechnology. 2021;19(1):1-24.

9. Khan A, Safdar M, Khan MMA, Khattak KN, Anderson RA. Cinnamon improves glucose and lipids of people with type 2 diabetes. Diabetes Care. 2003;26(12):3215-3218.
10. Tiwari P, Mishra BN, Sangwan NS. Phytochemical and pharmacological properties of Gymnema sylvestre: An important medicinal plant. Biomed Res Int. 2014;2014:830285.
11. Zhang L, Gu FX, Chan JM, Wang AZ, Langer RS, Farokhzad OC. Nanoparticles in medicine: Therapeutic applications and developments. Clin Pharmacol Ther. 2008;83(5):761-769.
12. Panyam J, Labhasetwar V. Biodegradable nanoparticles for drug and gene delivery to cells and tissue. Adv Drug Deliv Rev. 2003;55(3):329-347.
13. Reddy ST, Swartz MA, Hubbell JA. Targeting dendritic cells with biomaterials: Developing the next generation of vaccines. Trends Immunol. 2006;27(12):573-579.
14. Patel EK, Oswal RJ. Nanosponge and micro sponges: A novel drug delivery system. Int J Res Pharm Chem. 2012;2(2):237-244.
15. Sharma R, Pathak K. Polymeric nanosponges as an alternative carrier for improved retention of econazole nitrate onto the skin through topical hydrogel formulation. Pharm Dev Technol. 2011;16(4):367-376.
16. El-Say KM. Maximizing the encapsulation efficiency and the bioavailability of controlled-release cetirizine microspheres using Draper–Lin small composite design. Drug Des Devel Ther. 2016;10:825-839.
17. Kumar R, Pal A, Nayak AK. Development of chitosan-alginate microcapsules for colon-targeted delivery of flutamide: In vitro and in vivo characterization. J Pharm Pharmacol. 2013;65(5):567-577.
18. Patel DK, Kumar R, Prasad SK, Sairam K, Hemalatha S. Phytochemical and Pharmacological Properties of Gymnema sylvestre: An Important Medicinal Plant. Biomed Res Int. 2013;2013:1-12.
19. Subramanian S, Hussain MJ, Karuppannan SK, Saravanan M, Arunachalam KD. Effect of Solvent on the Phytochemical Extraction and GC-MS Analysis of Gymnema sylvestre. Pharmacogn J. 2020;12(4):1-7.
20. Sundarapandian S, Mohammed JH, Sathish KK, Saravanan M, Kantha DA. Effect of Solvent on the Phytochemical Extraction and GC-MS Analysis of Gymnema sylvestre. Pharmacogn J. 2020;12(4):1-7.
21. Khan A, Iqbal Z, Khan A, et al. Fourier Transform Infrared Spectroscopy Used in Drug-Excipients Compatibility Studies. Appl Spectrosc Rev. 2024;59(1):1-14.
22. Perlovich GL, Volkova TV, Bauer-Brandl A. Differential Scanning Calorimetry in Pharmaceutical Physical Chemistry. Mol Pharm. 2013;10(6):2217-2227.
23. Liu R, Langer R, Klibanov AM. Moisture-Induced Aggregation of Lyophilized Proteins in the Solid State. Biotechnol Bioeng. 1991;37(2):177-184.
24. Danaei M, Dehghankhold M, Ataei S, Hasanzadeh Davarani F, Javanmard R, Dokhani A, Khorasani S, Mozafari MR. Impact of particle size and polydispersity index on the clinical applications of lipidic nanocarrier systems. Pharmaceutics. 2018;10(2):57.
25. Baalousha M, Prasad A, Lead JR. Quantitative measurement of the nanoparticle size and number concentration from liquid suspensions by atomic force microscopy. Environ Sci Process Impacts. 2014;16(6):1338-1347.
26. Kumar R, Chandra A, Tomar PK. Synthesis and characterization of copper nanoparticles using Argemone mexicana leaf extract. Int J Nanomater Biostruct. 2014;4(3):66-71.

27. Mourdikoudis S, Pallares RM, Thanh NTK. Characterization techniques for nanoparticles: comparison and complementarity upon studying nanoparticle properties. Nanoscale. 2018;10(27):12871-12934.
28. Borchert H, Shevchenko EV, Robert A, Mekis I, Kornowski A, Grübel G, Weller H. Determination of nanocrystal sizes: a comparison of TEM, SAXS, and XRD studies of highly monodisperse CoPt3 particles. Langmuir. 2005;21(5):1931-1936.